Effect of binder on performance of intumescent coatings

Joana T. Pimenta, Carlos Gonç, alves, Loic Hiliou, Jorge F. J. Coelho, Fernão D. Magalhães

J. T.Pimenta, F.D.Magalhães
LEPAE, Departamento de Engenharia Química, Faculdade de Engenharia da Universidade do Porto, Rua Dr Roberto Frias, 4200-465 Porto, Portugal

C. Gonçalves
CIN - Corporação Industrial do Norte, S.A., Avenida Dom Mendo nº 831, Apartado 1008, 4471-909 Maia, Portugal

L. Hiliou
Institute for Polymers and Composites/I3N, University of Minho, Campus de Azurém, 4800-058 Guimarães, Portugal

J. F. J. Coelho
CIEPQPF, Department of Chemical Engineering, University of Coimbra, Polo II, Pinhal de Marrocos, 3030-790 Coimbra, Portugal

Abstract

This study investigates the role of the polymeric binder on the properties and performance of an intumescent coating. Waterborne resins of different types (vinylic, acrylic, and styrene-acrylic) were incorporated in an intumescent paint formulation, and characterized extensively in terms of thermal degradation behavior, intumescence thickness, and thermal insulation. Thermal microscopy images of charred foam development provided further information on the particular performance of each type of coating upon heating. The best foam expansion and heat protection results were obtained with the vinyl binders. Rheological measurements showed a complex evolution of the viscoelastic characteristics of the materials with temperature. As an example, the vinyl binders unexpectedly hardened significantly after thermal degradation. The values of storage moduli obtained at the onset of foam blowing (melamine decomposition) were used to explain different intumescence expansion behaviors.

Keywords Intumescent coatings, Binder, Thermal microscopy, Rheology

Introduction

Intumescent systems are a well-known and effective fire protection strategy.[1] In particular, intumescent coatings present relevant benefits, like ease of processing and application on several materials like plastics,[2] textiles,[3] metal,[4] and wood,[5] without modifying their intrinsic properties.[4] In the construction industry, intumescent coatings have gained particular relevance, especially for retarding the collapse of metal and wood structures, acting as a passive protection to allow the necessary time for safe intervention of rescue teams and building evacuation.[6,7]

When exposed to sufficiently high temperatures, intumescent coatings undergo significant expansion, forming a thermally insulating carbonaceous foam.[8] The three typical reactive components, responsible for the foaming and charring processes, are as follows: an acid catalyst source (ammonium polyphosphate— APP), a carbon source (pentaerythritol, PER), and a blowing agent (melamine, MEL). These compounds are bonded together by a polymeric resin,[9,10] forming a homogeneous film that can be applied by brushing or spraying. Titanium dioxide pigment is also present in the formulation, acting as an opacifier of the paint film and a reinforcing filler of the foam. Due to environ- mental concerns, the industry is nowadays mostly focused on the development of waterborne formulations.

In addition to the proportion of reactive components in the formulation, the performance of an intumescent coating is also affected by the type of polymeric binder.[11,12] This may be associated with different factors. In particular, the binder has an important contribution to the rheology of the molten medium that constitutes the coating at high temperatures. When the blowing agent decomposition starts, the rheological characteristics of the film will deter- mine the effectiveness of the foam expansion process.[13] In addition, the polymeric binder may also contribute to char formation, increasing the amount of thermally stable material in the insulating foam.[12] The choice of binder can therefore be a key issue in an intumescent coating formulation.

The present work studies the performance of intumescent coatings formulated with waterborne binders of different chemical natures: vinyl (copolymers of vinyl acetate and vinyl ester of versatic acid), acrylic, and styrene-acrylic resins. Previous studies in this area have been performed separately with epoxy, acrylic, and styrene polymers.[11,12,14,15] In the present work, the distinct polymeric binders are compared in terms of thermal stability and contribution to char formation. The formulated coatings are characterized in terms of intumescence development and thermal insulation performance. Thermal microscopy imaging and high- temperature rheology measurements provide complementary information that is fundamental for the understanding of the distinct fire protection performances observed for the different binder types.

Experimental

Materials and intumescent coatings preparation

The intumescent coatings followed the same formulation, as described in Table 1. All raw materials were provided by CIN S.A. (Maia, Portugal). The binder content was 25%, since this is representative of the value used in typical waterborne intumescent formulations.[16] Different waterborne vinylic and acrylic/styrene-acrylic resins were used as binders. Their chemical structure and the characterization data reported by the manufacturers are given in Table 2. The coatings were prepared in laboratory dispersers with Cowles type impellers and speeds ranging from 850 to 1200 rpm. The formulation components were added sequentially to the initial water, in order to insure maximum dispersion. The addition order was titanium dioxide, MEL, binder, PER, and APP. Special attention was taken to avoid overheating of the mixture, since this may induce premature degradation.

Characterization methods

A TG 209 F1 Iris (NETZSCH) was used for thermogravimetric (TG) analysis. The temperature range was from 20 to 900ºC, at a heating rate of 25ºC/min and under synthetic air flow (30 mL/min). Prior to analysis, the resins and coating samples were applied as films, dried, and broken into small pieces. About 10 mg of dry resins was used in the TG measurements. In the case of coatings, only about 5 mg was used to avoid over spilling of the intumescent foam during the measurement. Also for this reason, a special 6-mm high platinum crucible was used in this analysis.

A DSC 131 (Setaram) was used for differential scanning calorimetry (DSC) measurements. A heating rate of 5ºC/min under nitrogen gas (0.3 L/min) was used. As for TG, the samples were dried as films and then approximately 10 mg collected for analysis.

In order to evaluate intumescence development, 1-mm dry coating films were applied onto stainless steel plates (80 x 80 x 5 mm). Dry film thickness was confirmed with a MDC-1†SFB Digimatic Micrometer (Mitutoyo). Each coated metal plate (3 plates/coating) was placed into an electric furnace, being subjected to a heating rate of 50ºC/min during 15 min, followed by an isothermal step at 550ºC during 25 min. After cooling, the average thickness of the charred foam was monitored from 6 measurements in different points of each plate.

The thermal insulation performance of the intumescent coatings was evaluated on T-section steel structures (base: 10 9 13 cm, height: 13 cm, thickness: 1 cm). A 2-cm deep hole, 1.5 mm in diameter, was made on one of the vertical sides to allow insertion of a type K thermocouple. The coating films were applied on the T structures with a dry thickness between 750 and 850 1m. The film thicknesses were measured with a Surfix FN thickness gage (PHYNIX). The T structures were placed in a furnace and subjected to the temperature history shown in Fig. 1. This was recorded with a

thermocouple placed in the center of the furnace, i.e., at the same location as for the T structures. Only one structure was tested in each run, in order to avoid errors due to spatial temperature differences inside the furnace. An example of the appearance of a coated structure at the end of a run is shown in Fig. 2.

The temperature measured inside the T-section structures was recorded using a NI9211 24-bit thermo- couple input module (National Instruments) connected to a personal computer. The time at which a temperature of 500ºC was reached inside the T structure was recorded. This temperature is commonly used as reference, since it signals the loss in structural proper- ties of the material, impairing the load-bearing performance of steel beams.[17]

Thermal microscopy analyses were performed at Centro Tecnológico da Cerâmica e do Vidro (CTCV). Small samples of dry intumescent coatings with 3 x 3 x 0.2 mm were placed on a platinum crucible inside a tubular furnace and were subjected to a heating rate of 10ºC/min up to 900ºC. A Pt/Rh18 thermocouple recorded the temperature inside the furnace, close to the samples. The samples were illuminated indirectly with an optical mirror system. A video camera equipped with macro lens recorded the evolution of the sample during heating.

Scanning electronic microscopy (SEM/EDS) images of the intumescence surfaces were obtained at Centro de Materiais da Universidade do Porto (CEMUP), using a FEI Quanta 400FEG/Edax Genesis X4M system.

The rheological properties of binders were measured using an ARG2 stress-controlled rheometer (TA Instruments) equipped with parallel plates (diameter 25 mm). Disks cut from binders films prepared as indicated above were loaded in the preheated plates (100ºC) of the rheometer. The thermal and mechanical equilibrium of samples was monitored with the time evolution of the normal force and of the loss $(G\dagger)$ and storage $(G\prime)$ moduli recorded with small amplitude oscillatory shear (SAOS) at 1 Hz and a strain of 0.05 during 5 min. Then a temperature sweep with a rate of 1ºC/min was per- formed whereas both $G\prime$ and $G\dagger$ were recorded with SAOS performed at 1 and 10 Hz using a multifrequency scheme and a strain of 0.05. The thermal expansion of the shearing plates was automatically compensated by the rheometer, thus maintaining a constant gap of 1 mm. Fourier transformation of selected oscillatory torque signals exported after the tests indicated that data were recorded in the linear regime for the whole range of temperatures and that the temperature sweep was slow enough to allow the acquisition of sinusoidal torque data, thus confirming the visual inspection of oscillatory torque and strain recorded on-line.

Results

Thermal degradation

Figures 3 and 4 show the DSC thermograms obtained for all the studied resins. For the vinyl resins (Fig. 3), a main endothermic degradation peak is centered at about 315ºC.

Interestingly, a secondary peak is visible for VV1 at 240ºC, but is not apparent for VV2, even though it presents a broad peak that may be a combination of two individual degradation peaks. VV1 and VV2 are copolymers of vinyl acetate and vinyl ester of versatic acid monomers, while V1 is a vinyl acetate homopolymer. It can be hypothesized that the main peak, common to all resins, is associated with thermal decomposition of the vinyl acetate fraction, while the secondary peak, or the broadening of the main peak, is due to the presence of the versatic acid monomer in VV1 and VV2, respectively. Acrylic and styrene-acrylic resins, on the other hand, present thermal degradation peaks in the range 380 to 400ºC, indicating higher thermal stability than the previous set (Fig. 4).

Thermogravimetric analysis, shown in Fig. 5, con- firms the difference in thermal stability observed by DSC for the two resin groups. The vinyl resins present a major degradation step in the range from 280 to 400ºC. In agreement with the previous DSC observations, degradation starts at a lower temperature for VV1, about 240ºC, than for V1 and VV2. A second, less intense, mass loss stage is visible for all vinyl resins between 420 and 500ºC, and a third between 520 and 600ºC. This is in good agreement with the work of Rimez and co-workers on the thermal degradation of polyvinyl acetate.[18] Two main degradation steps were identified by those authors, which correlate well with the two first mass loss steps mentioned above. The first, most intense, occurred between 300 and 400ºC, and was shown to consist on a chain stripping process (deacetylation) combined with chain scission reactions at the end of the polymer chain. The product formed was identified as being a polyene (stable unsaturated material). Between 400 and 500ºC, a second degradation step was observed, consisting on the polyene chain scission.

The styrene-acrylic resins, EA1 and EA2, also presented in Fig. 5, show one main weight loss step between 340 and 450ºC. Acrylic resin A1 also decom- poses in one main step, at an intermediate temperature between the vinyl and the styrene-acrylic resins. Acrylic and styrene-acrylic resins are known to decom- pose mainly by chain scission mechanisms directly into volatile monomers,[19] instead of a two-step process as vinyl polymers.

The coating binder may contribute to the charred material if a stable product is obtained by interaction with APP.[4,12] This was investigated by thermogravimetry for mixtures of APP and the resins, in the same proportion as in the coating formulation. Figure 6 shows representative results obtained for VV2 and EA2. In the first case (Fig. 6a), the weight loss curve of the mixture is very close to the theoretical result (weighted sum of the individual decomposition curves for resin and APP). The resin decomposition product (a polyene, as previously discussed) is relatively stable and interaction with APP only seems to retard final decomposition (slightly more stable plateau between 500 and 600ºC). Similar results were obtained with VV1, V1, and A1. On the other hand, for the styrene-acrylic resins (Fig. 6b), the experimental curve is significantly above the theoretical one in the range 400–700ºC. This synergistic effect between styrene-acrylic copolymers and APP has been previously reported by Duquesne et al.,[12] being interpreted in terms of

reactions between substituted styrene and APP degradation products leading to entrapment of styrene monomers within the resulting phospho-carbonaceous structure.

Figure 7 shows the thermogravimetry results obtained for the formulated coatings. The weight loss stages can be related to the reactions that are known to play a part in this type of intumescent systems,[20–22] and are generically equivalent for all coating compositions tested. An initial weight loss step is found for all coatings between 200 and 300ºC, being associated with the onset of binder degradation and APP decomposition into phosphoric acid, releasing gaseous ammonia. In the ensuing stage, phosphoric acid reacts with PER between 280 and 350ºC to form polyol phosphates, which then decompose to char, releasing phosphoric acid, water, and ammonia. Within approximately the same temperature range (280–380ºC) MEL decomposes, producing ammonia and carbon dioxide. This set of reactions is responsible for the second weight loss step, and accounts for most of the gas production that originates intumescence expansion. Final decomposition of char and non- inorganic residues takes place above 600ºC, and only ceramic material remains in the end.

However, some relevant differences can be seen between the thermogravimetry curves corresponding to the two main groups of resins, vinylic, and acrylic/ styrene-acrylic. For the latter, the second weight loss step is visibly shifted to the right. The maximum weight loss rate occurs at 410ºC instead of 340ºC (Fig. 7), in agreement with the shift in thermal stability observed with the pure resins (Fig. 5). There is also a difference in the final (third) decomposition stage, where the vinyl coatings start losing mass at higher temperatures and at slower rates. This is probably due to the thermal insulation effect of the more expanded intumescence (discussed below) retarding decomposition of the material in the inner portions of the foam.

Intumescence morphology and thermal insulation

The results of char thickness tests performed on all coatings are shown in Tables 3 and 4. The coatings formulated with the vinyl resins yielded the higher thicknesses (Table 3). Coatings C_VV1 and C_VV2 show the highest expansions and uniformly developed foams. The coatings based on acrylic and styrene-acrylic resins developed very thin and compact intumescences, the best of which was obtained with resin A1.

Figure 8 shows SEM images of the surface of all the coatings after heating up to 500ºC. In agreement with the intumescence thickness results, the coatings that use vinyl binders show a well-formed foam-like structure underneath a thin superficial char film, with large cells uniformly distributed throughout the material. On the other hand, C_A1, C_EA1, and C_EA2 formed a compact char, with no visible foam cells.

The results of heat insulation tests performed with all coatings are shown in Fig. 9. All show similar behavior until a temperature between 200 and 250ºC. At this point, intumescence starts to develop and the temperature rises more slowly. C_VV1 and C_VV2 yielded the best results, showing the longer times to reach the critical

temperature of 500ºC (commonly adopted as the reference for loss of steel's load-bearing capability). The coatings performances decrease in the same order as the intumescence thickness decrease (Table 3). As expected, the volume of intumescence formed is the determinant factor for thermal insulation.

Thermal microscopy

Thermal microscopy has not been reported by other authors for studying intumescent systems; however, it can provide direct (visual) information about the foam development process. Figure 10 shows selected frames from the analysis performed on coating C_VV2 (vinyl- based coating). Some dilatation is visible at 200ºC (frame 1), but the material is still white. Above around 210ºC the coating starts to darken slightly, but no gas evolution is yet evident (frame 2). APP decomposition is the most relevant reaction taking place up to this point. At about 260ºC some expansion occurs, but fast foam growth starts only at about 280ºC, as MEL decomposes into gaseous products. Formation of small bubbles is now visible at the surface. At 300ºC the foam is expanding uniformly and rapidly (frame 3). Maximum expansion is reached at 327ºC and the sample is now homogeneously dark, being largely composed of charred material (frame 4). The foam then maintains its shape but contracts slowly until about 600ºC (frames 5 and 6), due to gradual slowdown of gas production until cessation at about 380ºC, and progressive decomposition of organic material. Finally, the foam starts to lighten (frame 7) until turning completely white at around 780ºC (frame 8), when only inorganic material is left. It is interesting to note that maximum expansion was attained at 327ºC (Fig. 10), which roughly corresponds to the temperature of maximum weight loss rate of the vinyl coatings (Fig. 7) and of the vinyl resins (Fig. 5).

Coating C_EA2 shows similar behavior in the initial stages (frames 1 and 2 in Fig. 11a), but after 280ºC a distinct phenomenon is observed. Substantial gas formation is visible, but uniform foam expansion does not occur. Gas accumulates within the film and surfaces as very large bubbles that grow until bursting, as illustrated in the frame sequence of Fig. 11b (frames 1–4). This process (large bubble growth and rupture) occurs until about 340ºC, after which the sample stabilizes (frame 4 in Fig. 11a), with a very small expansion relatively to original dimensions. The evolution up to 800ºC (not shown here) is similar to the observed in Fig. 10: slight contraction followed by whitening.

These results are consistent with the char thick- nesses observed for both groups of binders (Tables 3 and 4). The particular behaviors observed for each coating type will be used in combination with the rheology results described below to understand the different foam expansion processes.

Rheology

The distinct intumescence developments observed for the two groups of coatings cannot be clearly ascribed to the properties of the binders described so far. The onset of thermal degradation for the vinyl resins was close to the melamine decomposition temperature (280ºC), while it was significantly higher for the acrylic and styrene-acrylic resins. This may a priori indicate that the concomitance between resin decomposition and blowing agent decomposition is in some way beneficial for foam development. But any further conclusions are premature, because the efficiency of the foam expansion process depends directly on the viscoelastic character of the molten medium at the start of melamine decomposition. Since this is strongly influenced by the binder's rheological behavior,[12,23] the two resins previously selected for the thermal microscopy analysis, VV2 and EA2, were also used for rheological characterization.

As presented in Fig. 12, binder VV2 initially softens as temperature increases: the storage modulus decreases continuously until about 250ºC. Above this temperature, which is close to the previously identified onset of thermal degradation, $G\prime$ increases very sharply by three orders of magnitude until about 280ºC. Experimental noise becomes evident approaching 300ºC, caused by difficulty in maintaining constant strain due to the high elasticity of the sample. The dissipation factor, tan(δ), is higher than unity below 250ºC, indicating that the material is behaving as a viscoelastic liquid in the range of measured frequencies. However, it then drops significantly, showing a minimum at 270ºC, suggesting a liquid-to-solid transition. These increase in $G\prime$ and depression in tan(δ) past a certain temperature are unexpected. However, this rheological behavior can be explained considering the previously discussed formation of rigid polyene material from thermal degradation of the vinyl polymer, which is capable of undergoing crosslinking reactions. This results in a temperature-induced increase in rigidity, intensifying elastomeric behavior, and leading to a decrease in the dissipation factor. The fact that the temperature at which the material starts to harden is close to the onset of thermal degradation identified before for VV2 by thermogravimetric analysis (260ºC) reinforces this hypothesis. Even though the two types of measurements were performed at different heating rates, restricting direct comparisons when kinetic processes are involved, this agreement should not be considered coincidental.

The rheology data for binder EA2, on the other hand, show some distinct features (Fig. 13). Even though there is also an initial softening with temperature, up to 280ºC, this is followed by a plateau in $G\prime$, and no sharp increase is observed. The dissipation factor increases initially, alongside with the decrease in $G\prime$, and then shows a broad depression, starting at 280ºC. Decomposition occurs past 330ºC, originating a sharp decrease in $G\prime$.

In summary, the two binder materials show quite distinct rheological features. The first, VV2, behaves as a viscoelastic liquid until the onset of degradation at 250ºC, and

then develops elastomeric character and stiffens significantly due to crosslinking of degradation products. EA2, on the other hand, is a viscoelastic solid (since the dissipation factor essentially remains below 1 for the whole range of temperatures) with higher rigidity than VV2 in the lower temperature range, but then softens progressively until degradation. In the vicinity of 280ºC, when melamine decomposition initiates, the value of G_{ℓ} for EA2 is about two orders of magnitude lower in relation to VV2 (2 x 10^3 vs 3 x 10^4 Pa). Tan(δ), on the other hand, is roughly one order of magnitude higher (0.7 vs 0.01). The lower stiffness of EA2 at this temperature may be the key factor for the inefficient foam expansion. Growing gas bubbles rupture and coalesce within the molten medium, forming large gas pockets that end up surfacing and bursting, as observed in the thermal microscopy images. With VV2, on the other hand, bubble expansion is controlled by the more rigid elastic matrix. The gas formed is mostly retained in a uniformly distributed cell structure, allowing for homogeneous foam expansion as soon as melamine's blowing action starts.

Conclusions

This work evaluated the effect of the polymeric binder on the properties and performance of an intumescent paint formulation. A set of vinylic, acrylic, and styrene-acrylic waterborne resins were tested in the same paint formulation. Both the individual binders and the paints produced were extensively characterized.

Vinyl binders presented lower thermal decomposition temperatures than the acrylic and styrene-acrylic. This was verified both by calorimetric and thermo- gravimetric analysis. The thermal decomposition steps detected were in agreement with existing literature for each type of polymers. The acrylic and styrene-acrylic binders were seen to contribute to the formation of charred material, due to interaction of decomposition products with the ammonium polyphosphate catalyst present in the paint formulation.

Paint formulations with vinylic binders yielded very good intumescence development, while very low expansions were obtained with acrylic and styrene-acrylic paints. As a consequence, in the thermal insulation tests performed with steel structures, the first group yielded the best heat protection performance. Rheological analyses were performed on two binders representative of each group, in order to relate the observed development of the charred foams with the rheological features of the polymeric resins. The vinyl binder behaved as a viscoelastic liquid between 100ºC and the onset of degradation, at 250ºC. Surprisingly, at higher temperatures the material stiffened significantly, probably due to formation of unsaturated polymeric species from thermal degradation, as re- ported in literature, capable of undergoing crosslinking. The styrene-acrylic binder, on the other hand, behaved initially as a viscoelastic solid, but then softened progressively until degradation, above 320ºC. At 280ºC, when melamine starts decomposing into gaseous products, the styrene-acrylic binder presented significantly lower elastic rigidity than the vinyl polymer. This may hinder the uniform foam expansion of the paint

formulated with the first binder, due to rupture of growing foam cells, and consequent accumulation of gas into large pockets within the paint film. Thermal microscopy images collected between 280 and 300ºC for coatings formulated with both binders depicted foaming behaviors consistent with this hypothesis.

References

1. Bourbigot, S, Duquesne, S, "Fire Retardant Polymers: Recent Developments and Opportunities." *J. Mater. Chem.*, 17 2283–2300 (2007)

2. Horacek, H, Pieh, S, "The Importance of Intumescent Systems for Fire Protection of Plastic Materials." *Polym. Int.*, 49 1106–1114 (2000)

3. Horrocks, AR, Wang, MY, Hall, ME, Sunmonu, F, Pearson, JS, "Flame Retardant Textile Back-Coatings. Part 2. Effectiveness of Phosphorus-Containing Flame Retardants in Textile Back- Coating Formulations." *Polym. Int.*, 49 1079–1091 (2000)

4. Duquesne, S, "Intumescent Paints: Fire Protective Coatings for Metallic Substrates." *Surf. Coat. Technol.*, 180–181 302– 307 (2004)

5. Hassan, MA, Kozlowski, R, Obidzinski, B, "New Fire- Protective Intumescent Coatings for Wood." *J. Appl. Polym. Sci.*, 110 83–90 (2008)

6. Weil, ED, "Fire-Protective and Flame-Retardant Coatings—A State-of-the-Art Review." *J. Fire. Sci.*, 29 259–296 (2011)

7. Jimenez, M, Duquesne, S, Bourbigot, S, "Intumescent Fire Protective Coating: Toward a Better Understanding of Their Mechanism of Action." *Thermochim. Acta*, 449 16–26 (2006)

8. Nørgaard, KP, Dam-johansen, K, "Intumescent Coatings Under Fast Heating." *Eur. Coat. J.*, 6 34–39 (2012)

9. Wang, G, Yang, J, "Thermal Degradation Study of Fire Resistive Coating Containing Melamine Polyphosphate and Dipentaerythritol." *Prog. Org. Coat.*, 72 605–611 (2011)

10. Canosa, G, Alfieri, PV, Giudice, CA, "Hybrid Intumescent Coatings for Wood Protection Against Fire Action." *Ind. Eng. Chem. Res.*, 50 11897–11905 (2011)

11. Wang, G, Yang, J, "Influences of Binder on Fire Protection and Anticorrosion Properties of Intumescent Resistive Coating for Steel Structure." *Surf. Coat. Technol.*, 204 1186–1192 (2010)

12. Duquesne, S, Magnet, S, Jama, C, Delobel, R, "Thermo- plastic Resins for Thin Film Intumescent Coatings—Towards a Better Understanding of Their Effect on Intumescence Efficiency." *Polym. Degrad. Stab.*, 88 63–69 (2005)

13. Blasi, CD, Branca, C, Chimica, L, Li, F, "Mathematical Model for the

Nonsteady Decomposition of Intumescent Coatings." *AIChE J.*, 47 2359–2370 (2001)

14. Chuang, CS, Tsai, KC, Wang, MK, Ko, CH, Ing-Luen, S, "Impact of the Intumescent Formulation of Styrene Acrylic- Based Coatings on the Fire Performance of Thin Painted Red Lauan (*Parashorea* spp.) Plywood." *Eur. J. Wood Wood Prod.*, 67 407–415 (2009)

15. Drevelle, C, Duquesne, S, Le Bras, M, Lefebvre, J, Delobel, R, Castrovinci, A, Magniez, C, Vouters, MS, "Influence of Ammonium Polyphosphate on the Mechanism of Thermal Degradation of an Acrylic Binder Resin." *J. Appl. Polym. Sci.*, 94 717–729 (2004)

16. Kasten, NH, Groves, W, "Intumescent Fire Retardant Coating Compositions." US Patent 4,247,435, 1981

17. Han, Z, Fina, A, Malucelli, G, Camino, G, "Testing Fire Protective Properties of Intumescent Coatings by In-line Temperature Measurements on a Cone Calorimeter." *Prog. Org. Coat.*, 69 475–480 (2010)

18. Rimez, B, Rahier, H, Van Assche, G, Artoos, T, Biesemans, M, Van Mele, B, "The Thermal Degradation of Poly(vinyl acetate) and Poly(ethylene-co-vinyl Acetate), Part I: Experimental Study of the Degradation Mechanism." *Polym. Degrad. Stab.*, 93 800–810 (2008)

19. Beyler, C, Hirschler, M, "Thermal Decomposition of Polymers." In: DiNenno, P (ed.) *SFPE Handbook of Fire Protection Engineering*, 3rd ed., pp. 110–131. Quincy (2002).

20. Horrocks, AR, "Developments Inflame Retardants for Heat and Fire Resistant Textiles." *Polym. Degrad. Stab.*, 54 143– 154 (1996)

21. Wang, Z, Han, E, Ke, W, "Influence of Nano-LDHs on Char Formation and Fire-Resistant Properties of Flame-Retardant Coating." *Prog. Org. Coat.*, 53 29–37 (2005)

22. Wang, Z, Han, E, Ke, W, "Effect of Nanoparticles on the Improvement in Fire-Resistant and Anti-ageing Properties of Flame-Retardant Coating." *Surf. Coat. Technol.*, 200 5706–5716 (2006)

23. Anna, P, Marosi, G, Csontos, I, Bourbigot, S, Le Bras, M, Delobel, R, "Influence of Modified Rheology on the Efficiency of Intumescent Flame Retardant Systems." *Polym. Degrad. Stab.*, 74 423–426 (2001)
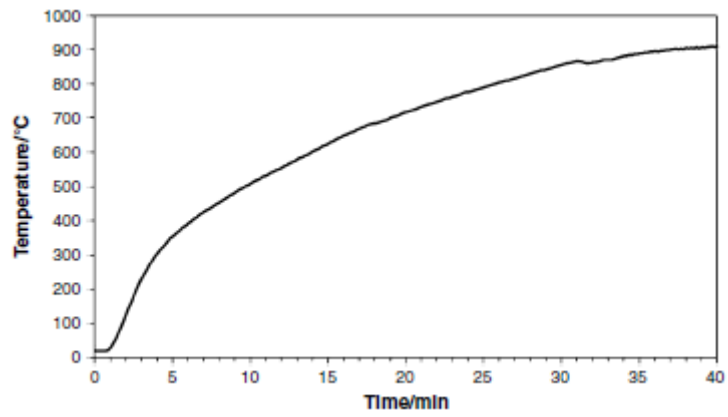
Fig. 1: Temperature history inside the furnace during a thermal insulation test

Fig. 2: Example of T steel structure inside the furnace after a thermal insulation test. Notice the white intumescent foam that remained on the structure
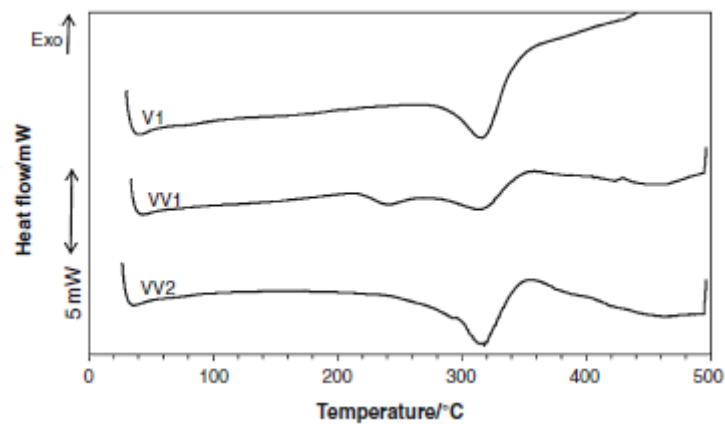
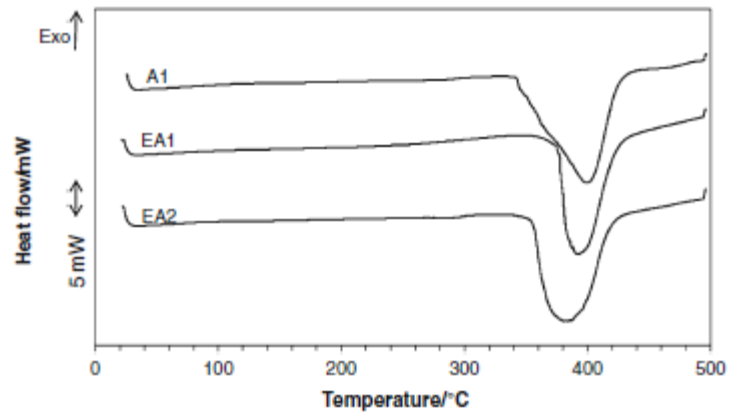

Fig. 3: DSC thermograms for resins V1, VV1, and VV2
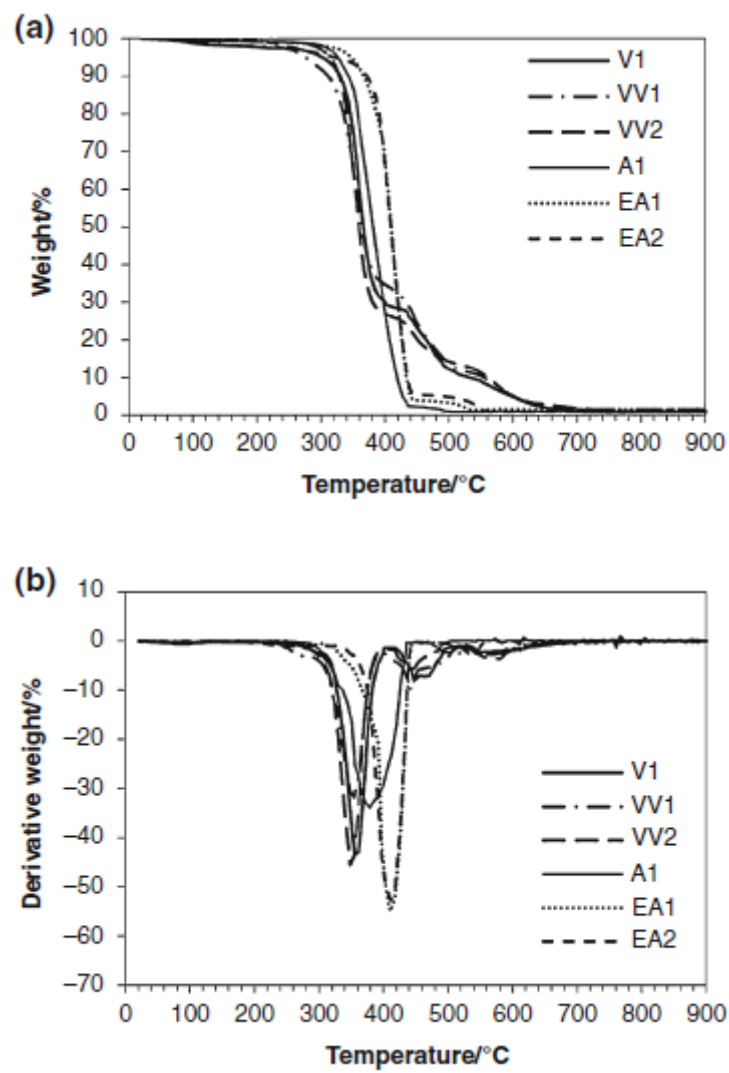
Fig. 4: DSC thermograms for resins A1, EA1, and EA2

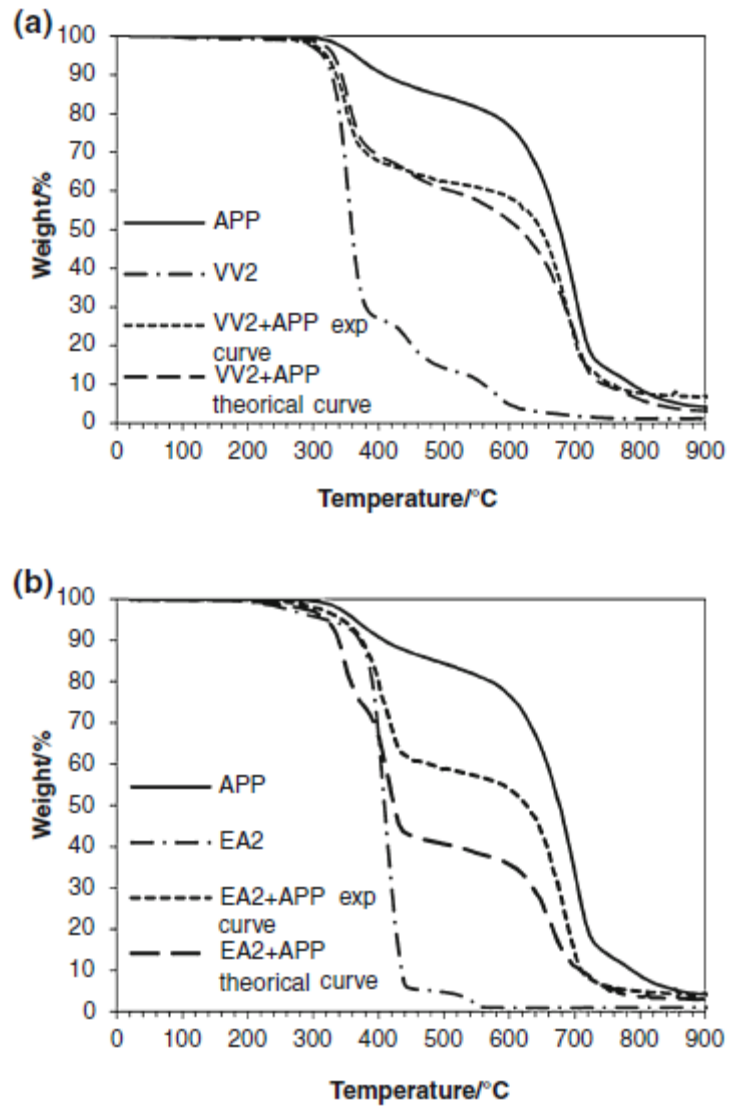Fig. 5: (a) TG curves for all resins studied. (b) First derivatives of TG curves

Fig. 6: (a) TG curves for VV2 + APP mixture and individual components. The ''theoretical'' curve corresponds to combination of V1 and APP curves. (b) Same as previous, for EA2 + APP mixture
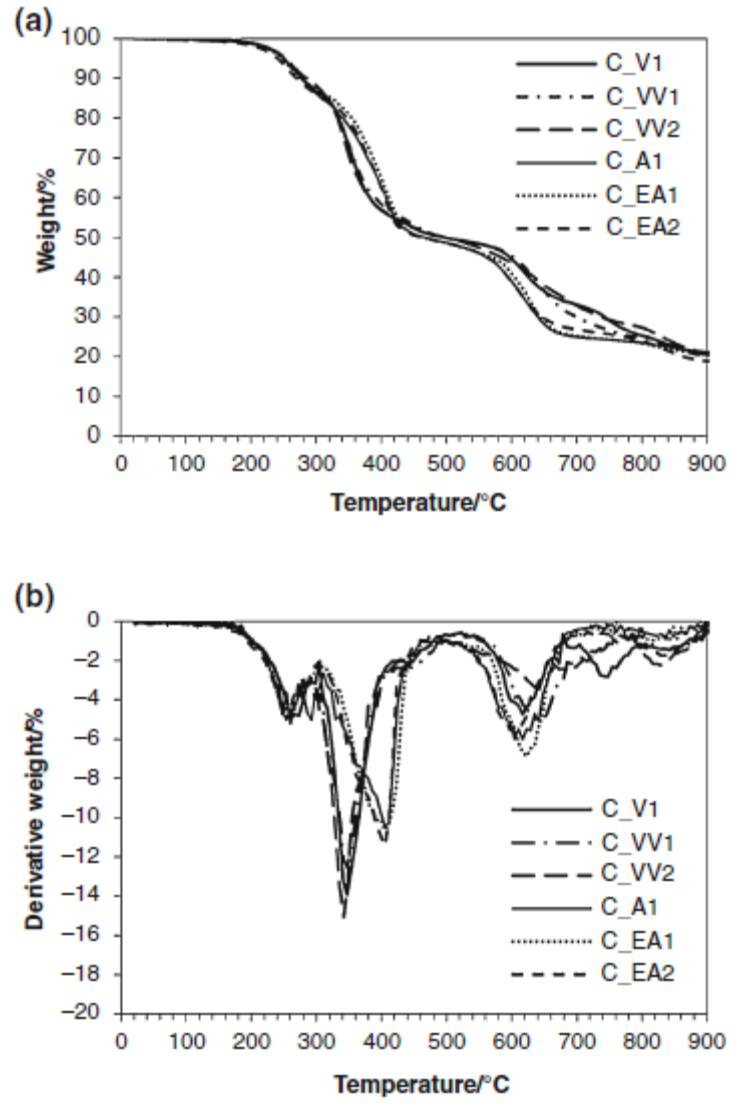
Fig. 7: (a) TG curves for the intumescent coatings studied. (b) First derivatives of TG curves
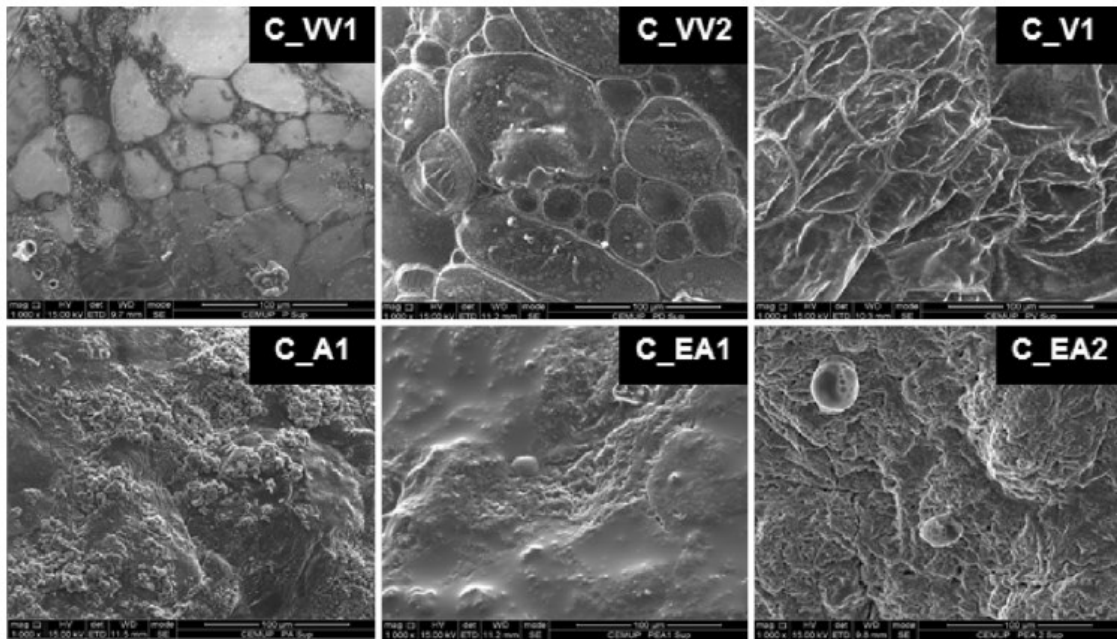
Fig. 8: SEM images of intumescence surface for the coatings studied (1000⤫ magnification)
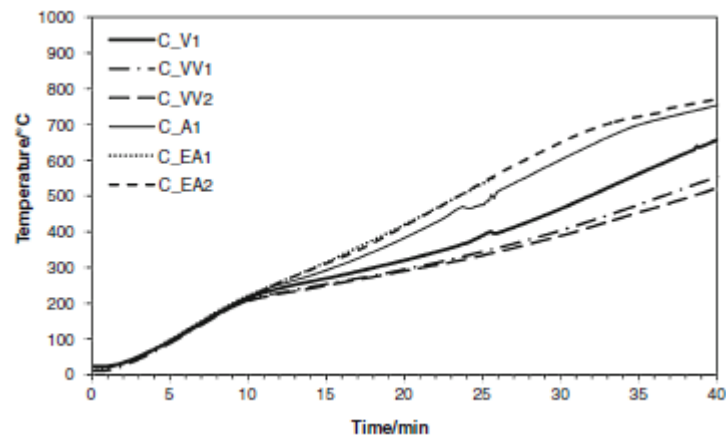
Fig. 9: Temperature history curves obtained in the thermal insulation tests
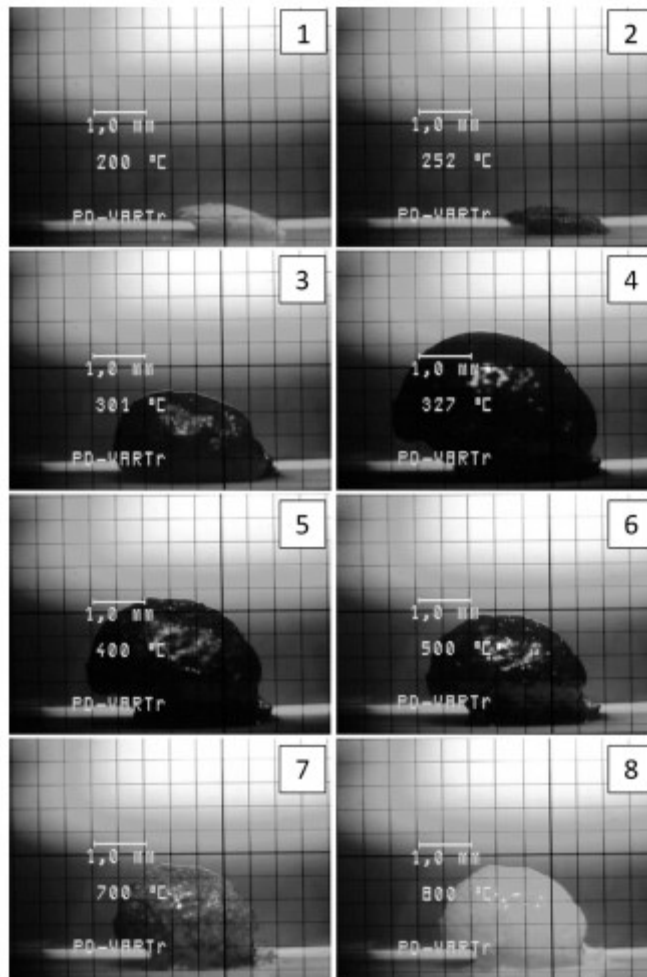
Fig. 10: Representative thermal microscopy images for c coating C_VV2 at different temperatures (1: 200ºC, 2: 252ºC, 3: 301ºC, 4: 327ºC, 5: 400ºC, 6: 500ºC, 7: 700ºC, 8:800ºC)
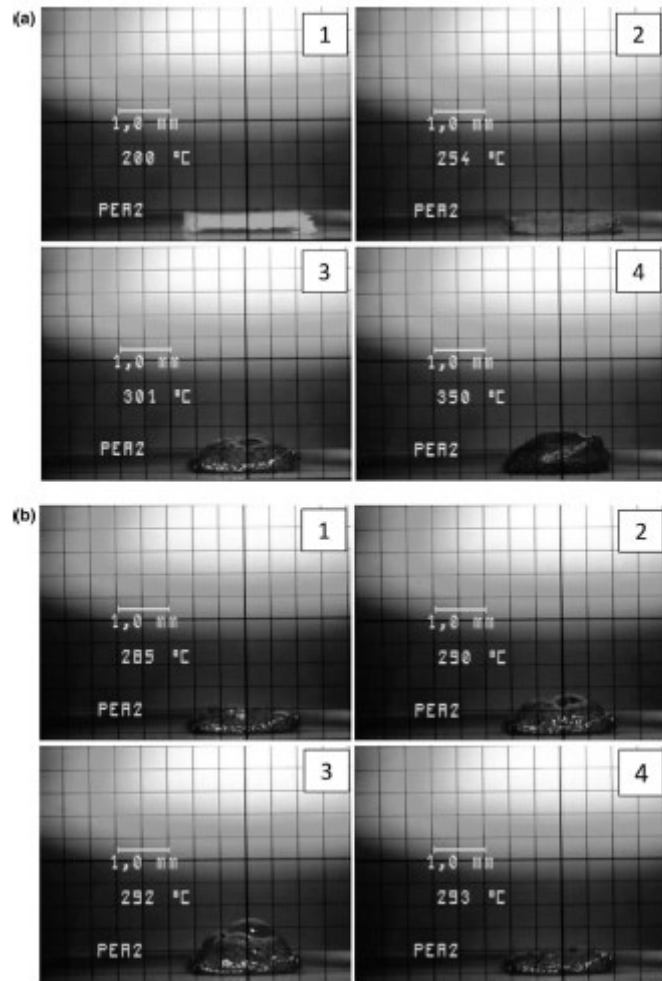
Fig. 11: (a) Representative thermal microscopy images for coating EA2 at different temperatures (1: 200ºC, 2: 254ºC, 3: 301ºC, 4: 350ºC). (b) Frame sequence exemplifying large bubble formation and collapse (1: 285ºC, 2: 290ºC, 3 and 4: 293ºC)
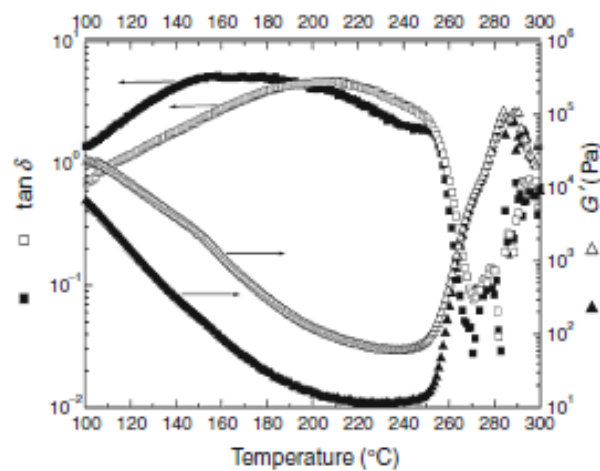

Fig. 12: Temperature dependence of phase shift angle δ and elastic shear modulus $G_\text{¢}$ for binder VV2, measured at 1 Hz (solid symbols) and 10 Hz (empty symbols)

Fig. 13: Temperature dependence of phase shift angle δ and elastic shear modulus G_t for binder EA2, measured at 1 Hz (solid symbols) and 10 Hz (empty symbols)
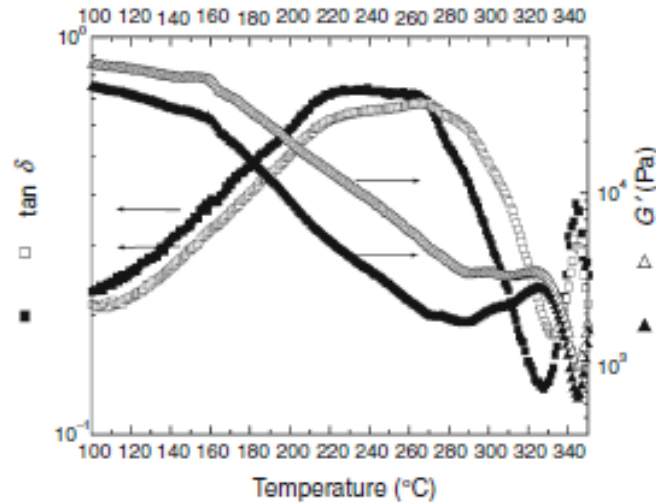
Table 1: Intumescent paint composition

Water (%)	TiO$_2$ (%)	MEL (%)	Resin (%)	PER (%)	APP (%)
25–30	5–10	5–10	20–30	5–10	20–25

Table 2: Polymeric resins used as binders in the intumescent coating formulations

Resin identification	Chemical composition of resin	Solid content (%)	Brookfield viscosity (mPa.s)	pH
VV1	Vinyl acetate–vinyl ester of versatic acid copolymer	49–51	3000–5000	4.0–5.0
VV2	Vinyl acetate–vinyl ester of versatic acid copolymer	49–51	2500–5000	3.5–4.5
V1	Vinyl acetate polymer	49–51	2500–5000	3.5–5.5
A1	Ester from acrylic and methacrylic acids copolymer	45–47	80–280	8.0–9.0
EA1	Butyl acrylate–styrene copolymer	49–51	700–1500	7.5–9.0
EA2	Ester from acrylic acid–styrene copolymer	49–51	750–1100	7.5–9.0

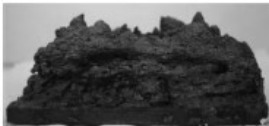Table 3: Char thickness test results for intumescent coatings obtained with resins V1, VV1, and VV2

Coating	C_V1	C_VV1	C_VV2
Char thickness (cm) Lateral view	2.4	4.2	5.2

Table 4: Char thickness test results for intumescent coatings obtained with resins A1, EA1, and EA2

Coating	C_A1	C_EA1	C_EA2
Char thickness (cm)	1.0	0.6	0.7
Lateral view			